Article

Not peer-reviewed version

Pseudo-Monthly Raman Lidar Data Set for Referenced Water Vapor Observations in the UTLS Domain

Dunya Alraddawi *, Philippe Keckhut, Guillaume Payen, Jean-Luc Baray, Florian Mandija, Abdanour Irbah, Alain Sarkissian, Michaël Sicard, Alain Hauchecorne, Helene Vérèmes

Posted Date: 17 February 2026

doi: 10.20944/preprints202602.1252.v1

Keywords: upper-tropospheric humidity; pseudo-monthly; Raman lidar; MLS-Aura; ERA5 reanalysis; GRUAN analysed radiosondes; water vapor mixing ratio

 doi:10.20944/preprints202602.1252.v1

Article

Pseudo-Monthly Raman Lidar Data Set for Referenced Water Vapor Observations in the UTLS Domain

Dunya Alraddawi [1,2,3,4,5,*], Philippe Keckhut [1,2,3,4,5], Guillaume Payen [5,6], Jean-Luc Baray [5,7], Florian Mandija [1,2,3,4,5], Abdenour Irbah [1,2,3,4,5], Alain Sarkissian [2,3,4,5], Michael Sicard [6], Alain Hauchecorne [1,2,5] and Helene Vérèmes [6]

[1] Laboratoire Atmosphères, Observations Spatiales (LATMOS), 11 Boulevard d'Alembert, 78280 Guyancourt, France
[2] Institut Pierre-Simon Laplace (IPSL), Observatoire de l'Université Versailles Saint Quentin, 11, Boulevard d'Alembert, 78280 Guyancourt, France
[3] Paris-Saclay University, 3 rue Joliot Curie, Bâtiment Breguet, 91190 Gif-sur-Yvette, France
[4] Sorbonne University, 21, rue de l'école de médecine, 75006 Paris, France
[5] Centre National de la Recherche Scientifique, 3 rue Michel-Ange, 75016 Paris, France
[6] Laboratoire de l'Atmosphère et des Cyclones (LACy), Météo-France, Université de la Réunion, Réunion, France
[7] Le Laboratoire de Météorologie Physique (LaMP), Université Clermont Auvergne, 63178 Aubière Cedex, France
* Correspondence: dunya.alraddawi@latmos.ipsl.fr

Highlights

A new Pseudo-monthly lidar water vapour mixing ratio dataset of 11 years record, is evaluated at subtropical upper-tropospheric altitudes, against MLS-Aura; ERA5; and GRUAN-analysed radiosondes humidity profiles. MLS systematically underestimate humidity relative to lidar especially above 12 km, while Lidar profiles are slightly drier than ERA5 and more importantly drier than radiosondes. An alternative lidar WVMR calibration would improve the lidar UT values.

What are the main findings?

- MLS and ERA5 underestimate subtropical upper-tropospheric water vapor compared to Raman lidar, with biases increasing above 12 km.
- Raman lidar shows a dry bias relative to radiosondes, partially linked to the GNSS-based calibration method.
- Alternative calibration of the lidar increases WVMR at the upper troposphere and improves consistency with radiosondes

What is the implication of the main finding?

- Improving the quality of Raman Lidar water vapour observation, and the consistency with radiosonde observations over the UTLS.
- Improving Satellites and re-analysis observations over the subtropics upper troposphere

Abstract

Upper Tropsphere (UT) humidity records are crucial for climat studies. Pseudo-monthly averaging is applied to maximize temporal representativeness, and enhance the lidar signal allowing to provide WVMR profiles up to 16 km. This study evaluates 11 years (2013–2023) of water vapor mixing ratio (WVMR) profiles from a UV Raman lidar (Lid1200) at the Reunion Island against MLS-Aura satellite retrieval, ERA5 reanalysis, and GRUAN-processed M10 radiosondes. Results show a systematic dry bias in MLS of up to 30% above 12 km, particularly during the wet season. Lidar exhibits a small underestimates of WVMR around 5% drier than ERA5 all over the UT, with the largest deviations above 14 km, and larger variability during the wet season, Lidar calibration-related challenges during the dry season results in drier than ERA5 WVMR profiles (up to 10%). Aditionnaly, comparisons with GRUAN-processed radiosonde reveal a substantial lidar dry bias, exceeding 100% above 12 km. Both lidar dry biases might be linked to the GNSS-based lidar calibration. Applying an alternative calibration method produces higher WVMR values, reducing the lidar dry bias w.r.t GRUAN by about 50% at upper-tropospheric levels, improving it's agreement with radiosondes, and revealing ERA5 dry bias increasing with altitude at the UT up to 25%. These efforts complement the global interest in the monitoring and validation of subtropical upper-tropospheric humidity.

Keywords: upper-tropospheric humidity; pseudo-monthly; Raman lidar; MLS-Aura; ERA5 reanalysis; GRUAN analysed radiosondes; water vapor mixing ratio

---

1. Introduction

Water vapor in the subtropical upper troposphere plays a central role in climate feedbacks and the radiative energy balance (IPCC, 2023). Small variations in humidity at these altitudes can have a disproportionately large impact on outgoing longwave radiation, making upper-tropospheric moisture one of the most sensitive amplifiers of climate change.

The Global Climate Observing System (GCOS) identifies upper-air water vapor as an Essential Climate Variable and prioritizes the reduction of observational gaps through improved data quality and long-term measurement capabilities (WMO, 2022). Improved observations also help constrain stratosphere–troposphere exchange processes, refine representations of moist convection in models, and reduce uncertainties in climate sensitivity projections [1–5].

A variety of techniques exist for measuring atmospheric water vapor—including in situ, ground-based, airborne, and satellite remote sensing [5,6]. Among these, spaceborne observations can provide global coverage across multiple atmospheric layers , but only few satellite instruments can reliably retrieve the vertical distribution of water vapor in the upper troposphere (UT) with sufficient accuracy and vertical resolution [7–9]

The Microwave Limb Sounder (MLS) [10] aboard NASA's Aura satellite, is a reliable tool for retrieving water vapor in the UT and lower stratosphere (LS). Despite the broad coverage and long-term continuity, MLS retrievals remain affected by uncertainties in humid and dynamically variable upper-tropospheric conditions. Comparisons with independent datasets [8,9,11,12] provide valuable insight into satellite performance, and this study contributes to these ongoing evaluation efforts, through the examination of 11 years (2013-2023) of its record over a sub tropical site.

In situ measurements from radiosondes provide valuable reference data, though those equipped with capacitive sensors are generally unreliable in the UT. Frost-point hygrometers, such as the Cryogenic Frost-point Hygrometer (CFH), offer superior accuracy, with uncertainties of 2–4 % in the tropical lower troposphere, 5–9 % near the tropopause, and approximately 10 % at 28 km [13,14]. CFHs have been used to assess subtropical humidity variability and trends [15], and to validate satellite-derived upper-tropospheric water vapor [13]. Nevertheless, their high cost and sensitivity to spatio-temporal mismatches limit routine deployment. Operational radiosondes, if robust against harsh conditions —as demonstrated by GCOS Reference Upper-Air Network (GRUAN)-certified instruments [16]—represent a promising alternative, though such data have only been available at Réunion Island since November 2019 and could not be validated previously (as far as we know). This study examine 4 years of GRUAN-analysed Meteomodem M10 radiosondes humidity at the UT (2019-2023)

Representing humidity at the UT remains a major challenge for atmospheric models [17]. ERA5 [18], the fifth-generation reanalysis from the European Centre for Medium-Range Weather Forecasts (ECMWF), provides long-term global information on upper-tropospheric moisture, but its uncertainties in this region can be questionned by radiosondes and satellites data being assimilated in. The hourly 37 pressure levels ERA5 dataset [19] will be also examined at the UT within the current study being available at the studied subtropical site for the same period.

Airborne in situ measurements further complement remote sensing. The IAGOS (In-service Aircraft for a Global Observing System; http://www.iagos.org, last accessed 31 January 2026) database provides H_2O observations from passenger aircraft, capturing strong vertical and temporal variability in the UT/LS over the extratropical Northern Hemisphere, while these data cover North America, the North Atlantic, and Europe (40–60° N), they are not available over the Reunion Island region [20].

Ground-based Raman lidars offer a highly reliable reference for upper-tropospheric water vapor, providing high vertical resolution and continuous WVMR profiles suitable for trend studies. Some NDACC systems, including Table Mountain Facility (United States) [21] and Tor Vergata (Italy) [22], and Observatory of Haute Province (France) [23], can reach UT altitudes, up to the lower tropopause in mid-latitude regions limits. At the edge of the tropical and subtropical latitude bands, a high-performance lidar has been operated at the Maïdo Observatory (2160 m a.s.l) since 2013 [24]. This system monitors water vapor from the surface to the LS and simultaneously measures stratospheric and mesospheric temperatures. Campaigns conducted since 2013 [22,25,26] demonstrated the lidar's ability to detect WVMR as low as a few ppmv in the UT/LS and to reach subtropical UT/LS altitudes through extended Raman integration [26]. Following this principle, The current study evaluates Pseudo-monthly means of Lid 1200 Raman Lidar Water vapour mixing ratio UT profiles over 11 years (2013-2023). This temporal screening allows the comparison to MLS retrievals, ERA5 outputs, and GRUAN-analysed radiosondes over the upper troposphere at the Reunion Island. Among our objectives, to provide insights into the reliability of these multi water vapor datasets at the UT and their applicability in climate and atmospheric studies, beside the evaluation of the Lidar dataset. Section 2 presents the Lid1200 lidar, Section 3 introduces all other datasets, Section 4 describes the comparison methodology with the main results, and we introduces an alternative Lidar calibration in Section 5 followed by conclusions.

2. The Raman Lidar

The Raman lidar has operated at the Maïdo Observatory on Réunion Island (21° S, 55.4° E) since 2012 [24]. The system was upgraded to a 355 nm emission wavelength, which provides more efficient Raman detection than the former 532 nm configuration. Laser pulses are produced by two Quanta Ray Nd:YAG lasers operating at 30 Hz. Using a dual-laser configuration significantly increases the emitted power; both lasers are synchronized with a pulse-generator module with a timing uncertainty below 20 ns. Each laser emits 375 mJ per pulse with a duration of 9 ns, and the beams are combined using a polarization cube.

The transmitter and receiver share a coaxial geometry. This configuration minimizes parallax effects, enables measurements down to the surface, and facilitates optical alignment. Backscattered photons are collected by a Newtonian telescope with a 1200 mm primary mirror, from which the system derives its designation "Lid1200."

Because Raman scattering from water vapor is much weaker than elastic backscatter, minimizing fluorescence sources in the detection chain is essential. Optical fibers are known to induce fluorescence that can introduce systematic biases in Raman measurements [27] ; therefore, no fiber is used in the system. Instead, an optical box is placed directly after the telescope to spectrally separate the Raman and Rayleigh returns. A diaphragm field stop at the entrance of this separation unit enables an adjustable field of view (FOV) ranging from 3 to 0.5 mrad. During routine operations, an FOV of 2 mm (0.5 mrad) is selected to reduce background light and prevent photomultiplier saturation from strong low-altitude elastic scattering. The overlap function is nearly identical for both Raman and elastic channels, allowing water vapor profiles to be retrieved down to the surface.

The spectral selection consists of a series of dichroic beam splitters and interference filters that separate the backscattered signal into its Raman and elastic components. Signal detection is performed using Hamamatsu miniature photomultiplier tubes (PMTs), and data acquisition relies on Licel transient recorders operating in photon-counting mode.

In addition to routine observations, the lid1200 system has participated in five intensive measurement campaigns, during which increased sampling frequency enabled extensive testing of various optical configurations. These efforts led to the selection of the current operational setup, as detailed in [22].

Water vapor mixing ratio profiles are derived from the ratio of Raman backscatter signals detected at 408 nm (water vapor; [27]) and 387 nm (nitrogen; [28]). These signals—recorded as photon counts per bin per laser shot—are corrected for background noise, adjusted for the differential atmospheric transmission T(z), and scaled by a calibration coefficient C.

The full processing chain, including uncertainty characterization and determination of the effective vertical resolution, is described in [26]. This study also examined the uncertainty associated with calibration using collocated GNSS-integrated water vapor (IWV) measurements. GNSS IWV accuracy is approximately 1 mm, corresponding to relative uncertainties of 6–18% depending on season and total atmospheric water vapor content.

Under routine operating conditions, the lidar system described in [22] provides water vapor profiles up to ~15 km. The primary limitations affecting retrievals near the tropopause and the detection of fine-scale UTLS structures—particularly in the presence of horizontal advection—arise from statistical uncertainties inherent to photon-counting detection. These uncertainties scale with the square root of the measured signal and depend on both vertical filtering and temporal averaging. Background noise also imposes significant constraints, which is why water vapor measurements from this Raman lidar are restricted to nighttime periods.

The native vertical resolution of the lidar measurements is 15 m. To reduce high-frequency noise, the profiles are smoothed using a low-pass filter based on a Blackman window, which provides sharp spectral filtering. Because noise increases with altitude, the number of smoothing points is increased with height to compensate for the reduced signal-to-noise ratio (SNR). The NDACC community has adopted two standard methods for defining the effective vertical resolution of lidar profiles: (i) the full width at half maximum (FWHM) of the finite impulse response [29], and (ii) the cut-off frequency of the digital filter, the latter being applied to the lid1200 data. Using the number of points employed in the Blackman filter at each altitude level, the corresponding vertical resolutions range from approximately 100–200 m in the lower troposphere, to about 500 m in the mid-troposphere, and around 600 m in the upper troposphere.

Longer temporal averaging of the Raman signals increases the lidar signal-to-noise ratio and therefore extends the usable altitude range of the WVMR profiles. [Vérèmes et al., 2019,26] demonstrated that a 10-minute integration typically provides reliable water vapor retrievals up to about 14 km, while 40-minute integrations allow the profiles to reach even higher altitudes. Following the same principle, we apply a pseudo-monthly integration strategy in which Raman signals are accumulated over several successive night-time periods within each month, yielding a total integration time of at least 1920 minutes. Figure 1 shows an exemple of one night WVMR profile which reaches about 14 km and the Pseudo monthly WVMR for the same month which reaches in turn more than 16 km. This newly built, Pseudo-monthly dataset offers a more suitable basis for comparisons with satellite measurements, and climatology studies. To further improve the robustness of the comparisons, all lidar data points for which the relative uncertainty exceeds 30% are excluded. Using this approach, we produce 100 pseudo-monthly WVMR profiles for the period 2013–2023, each with a vertical extent determined by its total accumulated signal.

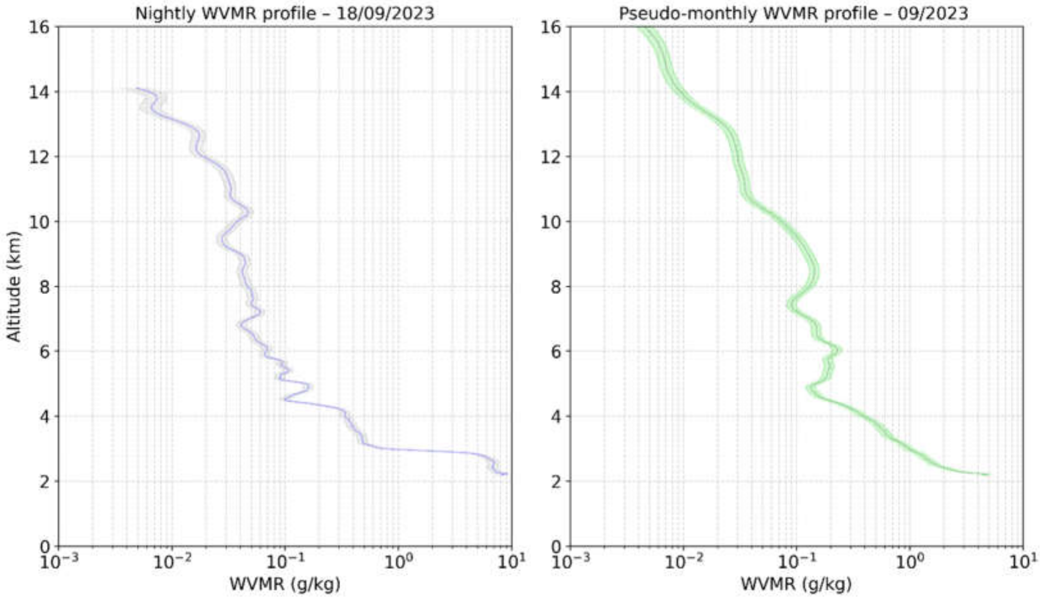

Figure 1. Lidar WVMR profile g/kg (Pseudo-monthly for September 2023: right panel, one night of 18/09/2023 :left pannel), errors shades are the lidar profile uncertaintity.

3. Other Evaluated Datasets

3.1. Microwave Limb Sounder MLS

The Earth Observing System Microwave Limb Sounder (EOS MLS; hereafter referred to as MLS), operating since July 2004 on the Aura spacecraft. MLS observed microwave radiances from the limb are inverted to profiles of temperature, geopotential height, cloud ice, and several minor gases, including water vapor mixing ratio from the upper troposphere (316 h.Pa) into the stratosphere [10]. MLS retrievals are spaced horizontally by 165 km [30] (1.5°) along the orbit track (roughly 15 orbits per day). The maximum MLS global retrieval rate is 3494 profiles per day. The spatial coverage is near-global (-82° to +82° latitude). The recommended useful vertical range is between 316 and 0.00215 hPa, and the vertical resolution is about 1.5 km at 316 hPa and 3.5 km at 4.64 hPa, and degrading to 15 km above 0.1 hPa.

The current study uses Version 5 in the Level 2 Geophysical Product (L2GP) files (MLS-Aura_L2GP-H2O_v05-00-c01) of water vapor retrievals publicly available at the Goddard Spaceflight Center DAAC through http://mls.jpl.nasa.gov. More information about this version via: https://mls.jpl.nasa.gov/data/v5-0_data_quality_document.pdf. We are following the recommended vertical range of data use as 316–0.001 hPa.

Biases in Aura MLS are well characterized globally, with multiple validation analyses of water vapour [8,12,31–35]

No previous studies validated multi years record of MLS over the Reunion island, our focus is evaluating water vapor mixing ratio (WVMR) profiles over the 10–16 km altitude range, corresponding to a vertical resolution of approximately 1.1 km, and a maximum horizontal shift of ~4° from the Maïdo Observatory (lidar location). To allow the comparison with the Lid1200 observations, only nocturnal MLS overpasses collocated with the lidar site —typically around 21:00–22:00 local time— are considered. From these, 76 pseudo-monthly MLS WVMR profiles were generated for comparison with coincident lidar measurements between 2013 and 2023. Two examples of one night WVMR profile and the pseudo monthly WVMR for the same night month over the subtropical upper troposphere site are presented in Figure 2.

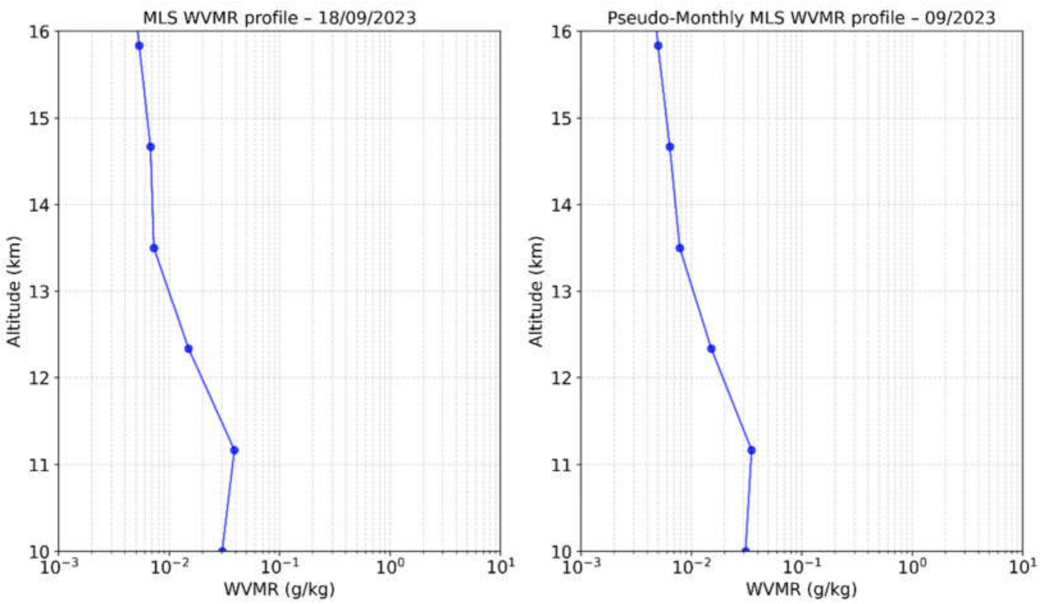

Figure 2. WVMR profiles g/kg from MLS-Aura Satellite (Pseudo-monthly for September 2023: right panel, Mean of overpasses of the night of 18/09/2023 :left panel), over the 10 to 16 km altitudes. Errors shades are the profile uncertaintity which are too small to be visible (< 5% mostly).

3.2. ERA5 Re-Analysis

ERA5 is the fifth generation of the atmospheric meteorological reanalysis produced by the European Centre for Medium-Range Weather Forecasts (ECMWF), which is operational since 2016 [18]. ERA5 benefits from a decade of developments in model physics, core dynamics and data assimilation to guide and readjust the outputs of interactive models. ERA5 used dataset [19] has a significanlty enhanced horizontal resolution of 31 km (0.25°), compared to 80 km for the previous reanalysis (ERA-Interim), hourly output over 37 pressure levels, and provides a detailed publicly available record of the global atmosphere from 1979 onward (and with less frequent data between 1950-1979). Uncertainty spread of tropospheric humidity samples, mainly random errors, decreases over time. Relative spread is lowest near the surface (5%), but around 15% for specific humidity at 300 h.pa since 2015 [18]

WVMR is calculated using the specific humidity variable at the nearest ERA5 pixel to the lidar location, i.e Maido Observatory. To match the lidar observations, data are selected with a maximum horizontal (spatial) drift of 0.1° and the best temporal coincidence with nighttime lidar measurements. Using this approach, 91 pseudo-monthly ERA5 WVMR profiles are retrieved for the 2013-2023 period to enable direct comparison with the lid1200 ones. Two exemples of WVMR profiles of one lidar-like night and lidar-like month (pseudo) are presented in Figure 3.

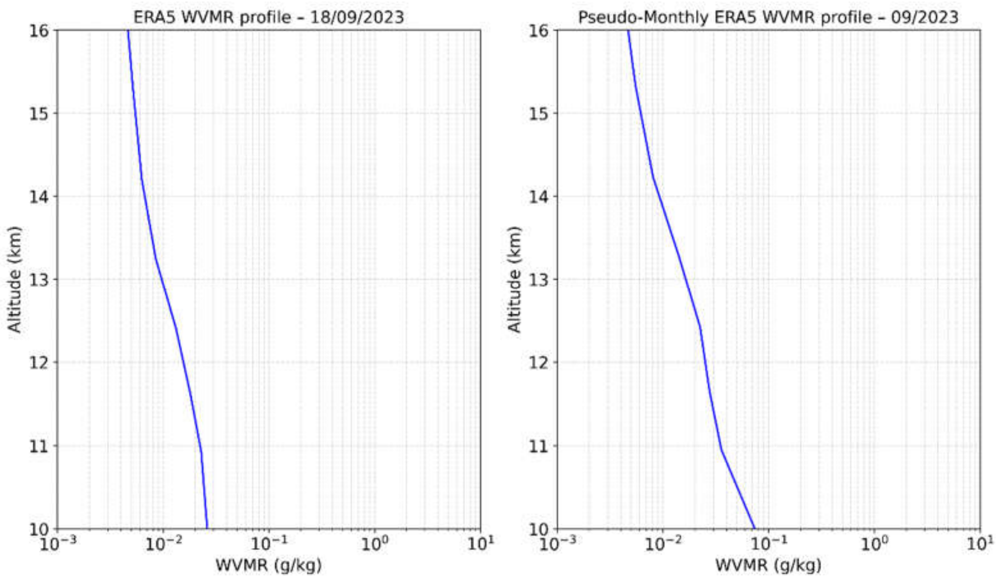

Figure 3. WVMR profiles g/kg from ERA5 (Pseudo-monthly for September 2023: right panel, Lidar-like night of 18/09/2023 :left panel), over the 10 to 16 km altitudes.

3.3. GRUAN-Processed Meteomodem M10 Radiosondes

Balloon borne radiosondes provide local humidity profiles above the launch site, although spatial collocation with fixed-point measurements can be affected by wind speed and direction at altitudes where the ballons drifts. By approximative location to the lidar, we choosed the Gillot meteorological station (also referred to as Chaudron in the data files, WMO code for this Meteo France station: 61980) in Saint-Denis port (20.9°S, 55.5°E, 46 m asl) where Meteomodem Co. (www.meteomodem.com) M10 radiosondes are regularly launched at midnight and midday. Towards reference-quality and hence better climate-quality measurements, this station's radiosonde dataset benefit from regular processing, applied and coordinated by the GRUAN (GCOS Reference Upper-Air Network, https://www.gruan.org/) [36] to provide well-calibrated water vapour measurements. Where few corrections are applied to M10 radiosondes data to meet the (GRUAN) standards [36], these corrections are detailed in [Dupont et al., 2020,37], including: (1) calibration adjustements; (2) corrections for slow sensor response particularly at extreme humidity; (3) compensation for relative humidity sensor dependence on temperature gradients; and (4) time-lag corrections at cold temperatures which affects measurements in regions with strong relative humidity gradients.

WVMR profiles (involved in the current study) are retrieved using the corrected relative humidity (all corrections applied) [37], air temperature and pressure levels of M10 radiosondes midnight launches. So, between November 2019 and December 2023, 41 GRUAN-processed M10 WVMR profiles were retrieved and compared with coincident lidar measurements at a pseudo-monthly scale. Figure 4 shows two examples of a midnight launch WVMR profile and a pseudo-monthly profile.

A first look at both WVMR profiles, would show much higher UT values compared to those retreived by ERA5 (Figure 3), MLS (Figure 2), or even lidar (Figure 1). Here after we carried out a statistical comparison to get more insights.

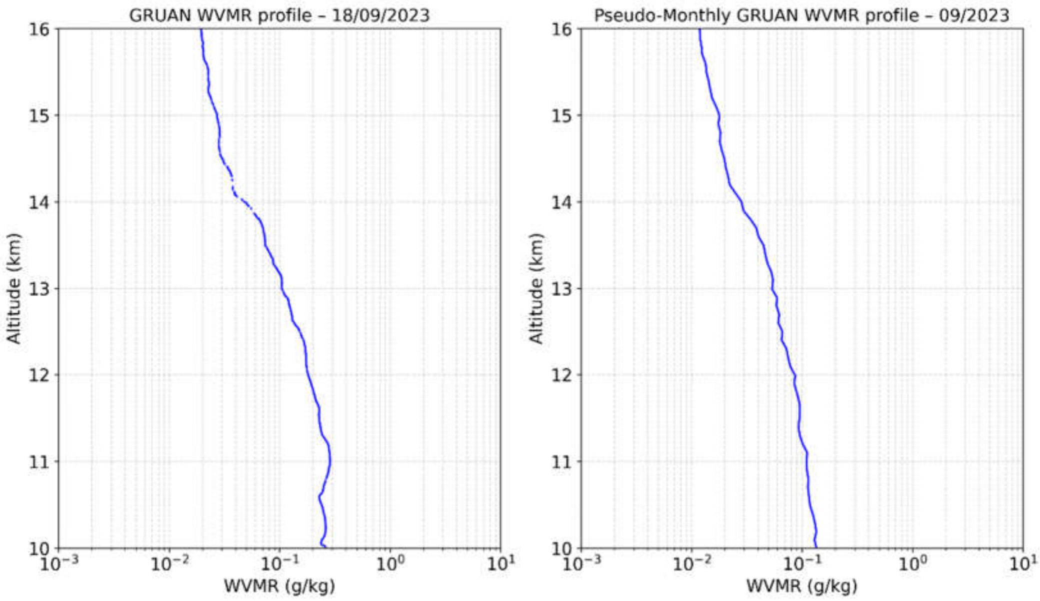

Figure 4. WVMR profiles g/kg from GRUAN-processed M10 radiosonde (Pseudo-monthly for September 2023: right panel, night of 18/09/2023 : left pannel), over the 10 to 16 km altitudes.

4. Lidar Bias to Others at the Upper Troposphere

A central challenge of this study is the limited number of true nocturnal lidar-like satellite overpasses suitable for direct comparison of WVMR profiles. The pseudo-monthly WVMR dataset generated from Lidar, MLS, ERA5, and GRUAN nocturnal observations would overcome such a constraint. This temporal aggregation maximizes the number of usable MLS ovserpasses, also it improves the robustness of comparisons in the upper troposphere, while taking advantage of the lidar's capability to probe higher altitudes through long-duration Raman signal accumulation. All comparisons are performed with respect to the Raman Lidar, and relative differences are used to characterize the uncertainties of each dataset. Inevitably, gaps occur in the pseudo-monthly time series, mainly during periods without valid observations (missed profiles due to instrument downtime or COVID-19 pandemic disruptions, or profiles didn't meet the quality criteria selection having errors > 30%).

4.1. LIDAR vs. MLS-Aura

Relative differences between the lidar and MLS water vapor mixing ratio profiles were examined over the useful 10–16 km altitude range, where both instruments provide robust measurements. For each month, all MLS observations coincident with lidar night-time measurements were averaged to form a representative pseudo-monthly profile. Over the 2013–2023 period, this procedure yielded 76 pairs of lidar–MLS pseudo-monthly profiles, all are having the MLS vertical resolution.

The median relative difference in WVMR between the lid1200 lidar and MLS over the 11-year period is shown in Figure 5 (black dashed line), together with the 95% confidence interval of the variability (blue shading). The confidence bounds are calculated as ±2 times the pseudo–standard error, normalized by the square root of the number of contributing profile points in each altitude bin. Differences are smallest between 11 and 12 km, but the lidar reports values up to 30% higher at altitudes above this layer. The spread increases above 14 km, consistent with reduced lidar sensitivity and the coarser MLS vertical resolution at higher altitudes. This dry MLS bias in the upper troposphere is consistent with previous investigations [8,32], and similar magnitudes have been reported over Reunion Island in earlier lidar–satellite shorter terme comparisons (e.g Dionisi et al., 2015) [22].

 doi:10.20944/preprints202602.1252.v1

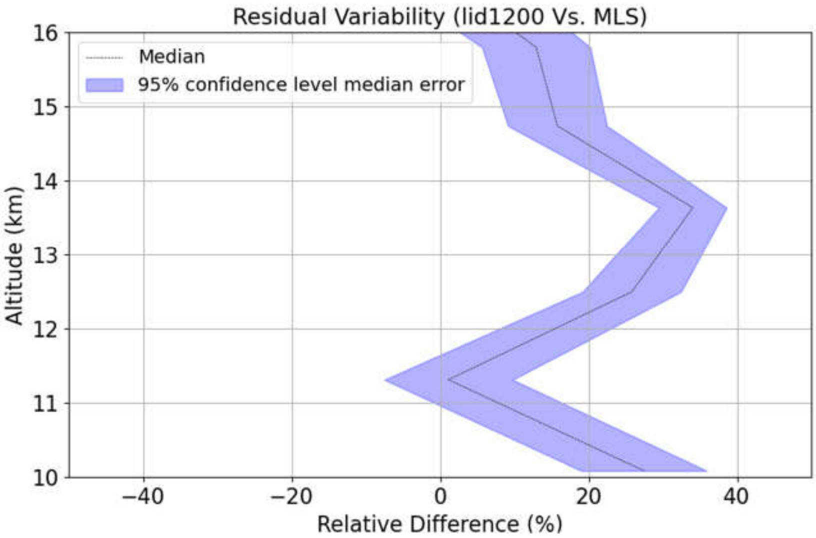

Figure 5. Median Lidar WVMR relative bias (%) w.r.t MLS (over 76 compared profiles from 2013 to 2023), shaded zones refine the 95% confidence level of the relative error.

Hereafter we investigate the temporal evolution of the relative differences (Lidar - MLS) for the whole period at two distinguished altitude levels (Figure 6); at 11.3 km and at 13.7 km altitude levels, where different magitude of the median bias (Figure 5) is reported. We observe significant interannual variability, at 13 km (blue bars): the relative differences refer to a dominant MLS dry bias (Lidar > MLS); at 11 km (red bars) the differences are also substantial but show a slightly more stable trend around 0%, though extreme peaks persist. Dominant MLS dry bias is observed at both altitudes during 2018 & 2019.

Some gaps in data correspond to periods where coincident MLS and lidar observations were insufficient to generate a representative MLS-Lidar pseudo-monthly deuo profiles (only one night of observation during the month for example)

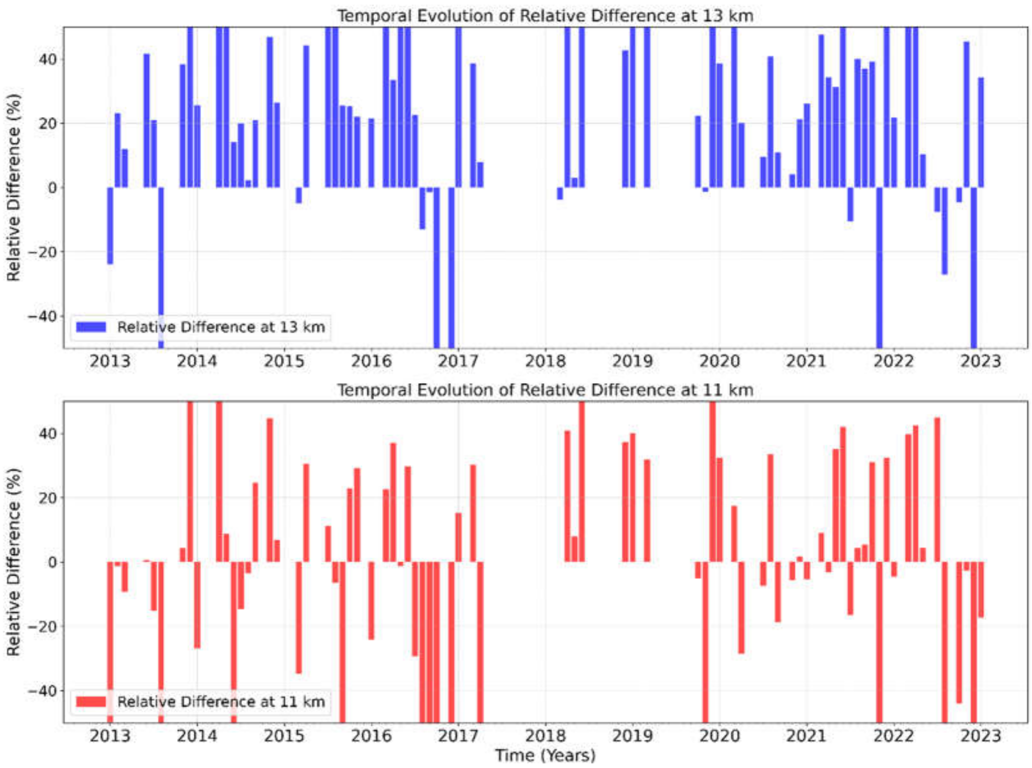

Preprints.org (www.preprints.org) | NOT PEER-REVIEWED | Posted: 17 February 2026 doi:10.20944/preprints202602.1252.v1

Figure 6. Temporal evolution of relative differences (%) between lidar and MLS (Lidar – MLS) at 13 km (bleu) and 11 km (red) altitudes from 2013 to 2023. Positive values indicate that lidar reports higher WVMR than MLS. Gaps correspond to months with insufficient coincident data.

To further investigate seasonal influences, the analysis was separated into two main subtropical seasons: a dry season (May–September) and a wet season (October–April). The relative differences exhibit a distinct structure during the wet season (Figure 7-a) with clear MLS dry bias, would reach 40% between 12 and 14 km. This may reflect improved lidar sensitivity under moister conditions, which reduces calibration-related limitations and enhances the effective lidar performance in the upper troposphere. MLS dry bias is still observed during the dry season (Figure 7-c) all over the UT altitudes except around 11km where the relative differences show a slightly more stable trend around 0%. The smaller magnitude of MLS dry bias w.r.t lidar during the dry season could be attributed to mutual complications of water vapor measurements during such dry conditions, see Figure 7 (b and d for median WVMR profiles during the wet and dry season respectively, all analysis are carried out over the 2013-2023 (11 years) period.

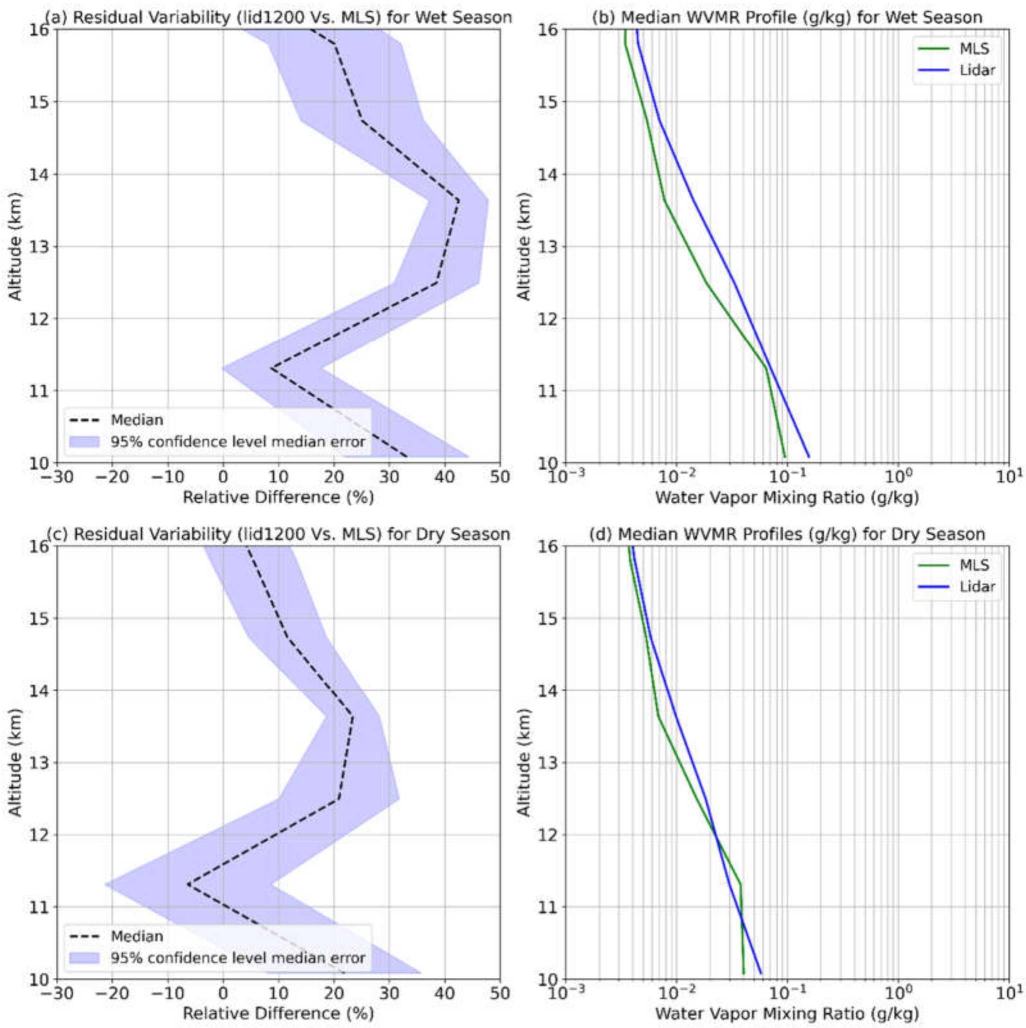

Figure 7. (a) Median Lidar WVMR relative bias (%) w.r.t MLS during wet season months, (b) Median WVMR profile during the wet season (g/kg), (c) Median Lidar WVMR relative bias (%) w.r.t MLS during dry season months, (d) Median WVMR profile during the dry season (g/kg) , all over the 2013 to 2023 study period. Shaded zones refine the 95% confidence level median error.

 doi:10.20944/preprints202602.1252.v1

4.2. LIDAR vs. ERA5

The relative differences between lidar-derived WVMR and ERA5 reanalysis were evaluated also on a pseudo-monthly basis over the subtropical site. For each month, ERA5 hourly profiles coincident with lidar nighttime measurements were averaged to construct a representative pseudo-nightly profile, then a pseudo-monthly one. The comparison focuses on the 10–16 km altitude range. Over the 2013–2023 period, a total of 91 pseudo-monthly WVMR profiles were produced. The overall lidar-to-ERA5 bias is summarized by the median of the 91 relative-difference profiles. ERA5 shows a small wet bias relative to the lidar, and would reach around 5% (Figure 8). We further zoomed on the temporal evolution of the relative differences (Lidar - ERA5) for the whole period at two distinguished altitude levels (Figure 9); at 11km and at 14km altitude levels, where slightly different magitude of the median bias (Figure 8) is reported. Again, positive values indicate a dry bias in ERA5 and negative values indicate a wet bias: (blue bars): the relative differences refer to a dominant ERA5 wet bias (Lidar < ERA5) mostly before 2018 but the total median was mostly affected by enhanced variability along the years after 2018 resultitng in a median bias around 0% (Figure 8). At 11 km, Lidar values seemed mostly drier up to 2021, and the bias seemed to be inversed after that (red bars) resulting in a slight small Lidar dry bias w.r.t ERA5 up to 5%.

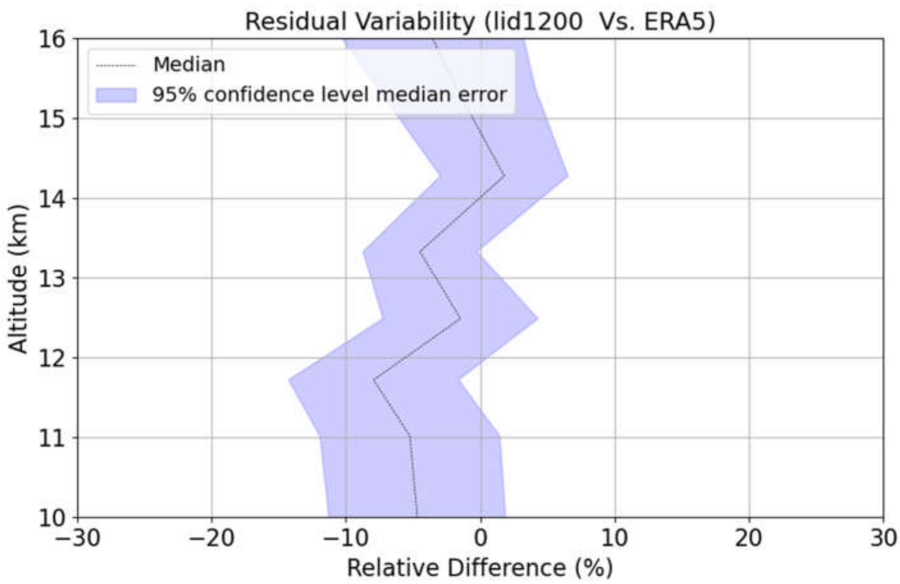

Figure 8. Median Lidar WVMR relative bias (%) w.r.t ERA5, (over 100 compared profiles from 2013 to 2023) shaded zones refine the 95% confidence level of the relative error.

 doi:10.20944/preprints202602.1252.v1

Figure 9. Temporal evolution of relative differences (%) between lidar and ERA5 (Lidar – ERA5) at 14 km (bleu) and 11 km (red) altitudes from 2013 to 2023. Positive values indicate that lidar reports higher WVMR than ERA5. Gaps correspond to months with lidar missed data.

The analysis was further separated into the two dominant subtropical seasons, revealing distinct patterns in the relative differences between lidar and ERA5. During the wet season (Figure 10-a), ERA5 small dry bias of 5% seemed to persisit at the upper altitudes, above 14 km: ERA5 bias w.r.t lidar could be attributed to model assumptions in ERA5 at the upper troposphere ; while the variability of the bias is generally larger below 14 km, where lidar values tends to get drier than the ERA5 ones (up to 10%). This variability may reflect calibration-related lidar uncertainties, More evident during the dry season (Figure 10-c), throughout the profile. The seasonal median of both datasets are presented in Figure 10 (b and d for median WVMR profiles during the wet and dry season respectively), all analysis are carried out over the 2013-2023 (11 years) period.

doi:10.20944/preprints202602.1252.v1

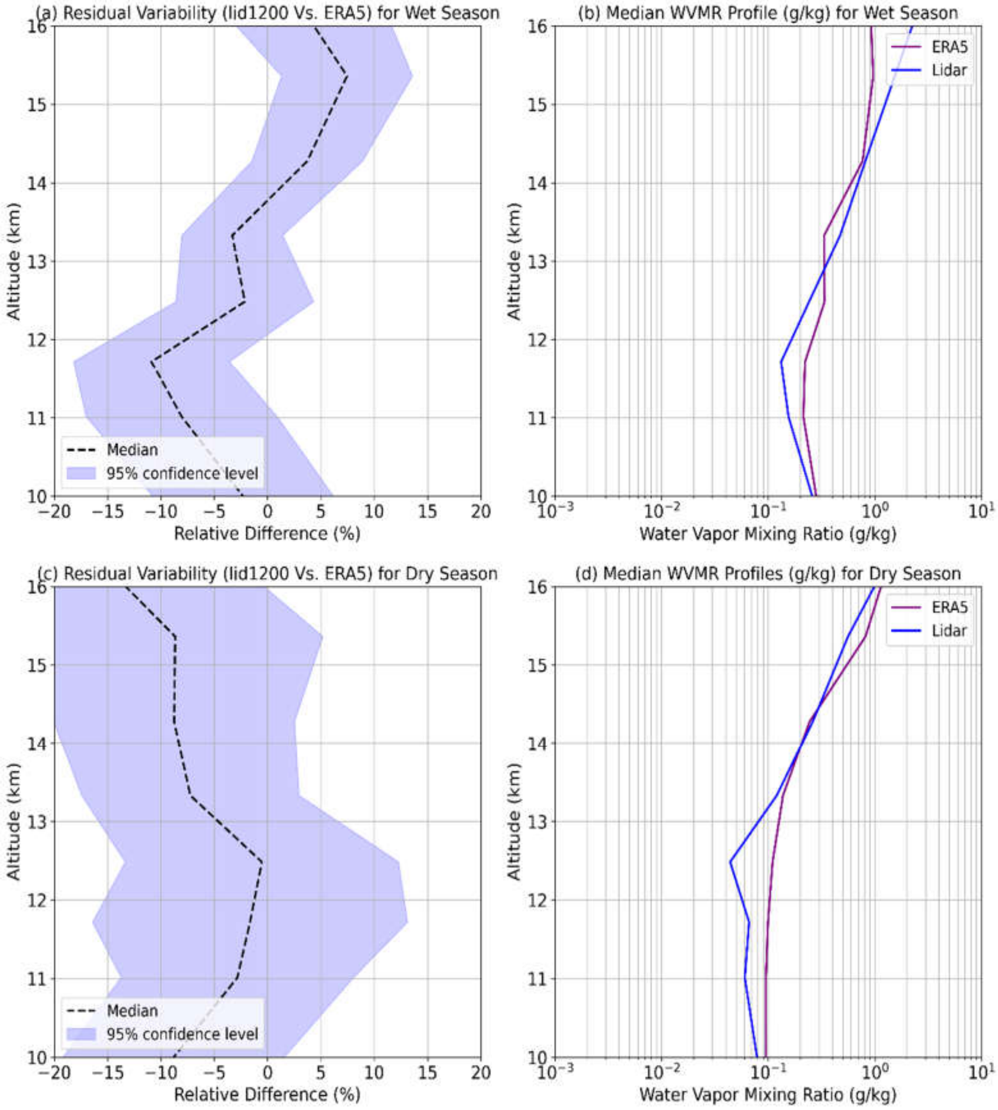

Figure 10. a) Median Lidar WVMR relative bias (%) w.r.t ERA5 during wet season months, (b) Median WVMR profile during the wet season (g/kg), (c) Median Lidar WVMR relative bias (%) w.r.t ERA5 during dry season months, (d) Median WVMR profile during the dry season (g/kg) , all over the 2013 to 2023 study period. Shaded zones refine the 95% confidence level median error.

4.3. LIDAR vs. GRUAN-Processed M10 Radiosondes

The relative differences between lidar-derived WVMR and GRUAN-processed M10 radiosondes were also evaluated on a pseudo-monthly basis. For each month, all GRUAN midnight soundings coincident with lidar nighttime measurements were averaged. The comparison focuses on 10–16 km over the 2019–2023 period, during which 41 pseudo-monthly profiles were retrieved. The lidar bias relative to GRUAN is defined as the median of all relative-difference profiles. In contrast with previous subsections, the lidar exhibits a pronounced dry bias, exceeding 100% above 12 km and approaching 200% near and above 13 km, while remaining around 60% below 11 km (Figure 11) and decrease towards the lower troposphere (not shown). Getting such a clear bias magnitude, we didn't investigate further the temporal evolution of the relative differences.

Seasonal stratification reveals clear differences between the wet and dry periods (Figure 11). During the wet season, the variability is larger, with biases frequently surpassing 200% above 12 km. Enhanced column humidity may increase Raman backscatter strength, improving upper-tropospheric sensitivity, but spatial mismatch between the radiosonde ascent and the lidar location—

especially when trajectories drift toward the southwest Indian Ocean—can also amplify discrepancies. During the dry season, the median bias is reduced, approximately 40% below 11 km and rising to 100% between 12 and 13 km, reaching up to 150% at higher altitudes. The extremely dry wintertime conditions further complicate lidar calibration, contributing to the observed deviations.

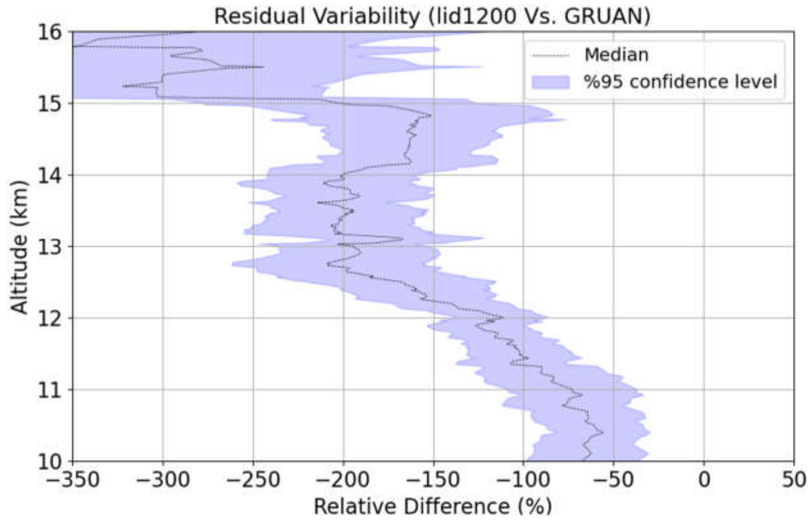

Figure 11. Median Lidar WVMR relative bias (%) w.r.t GRUAN M10, (over 41 compared profiles from 2019 to 2023), shaded zones refine the 95% confidence level of the relative error.

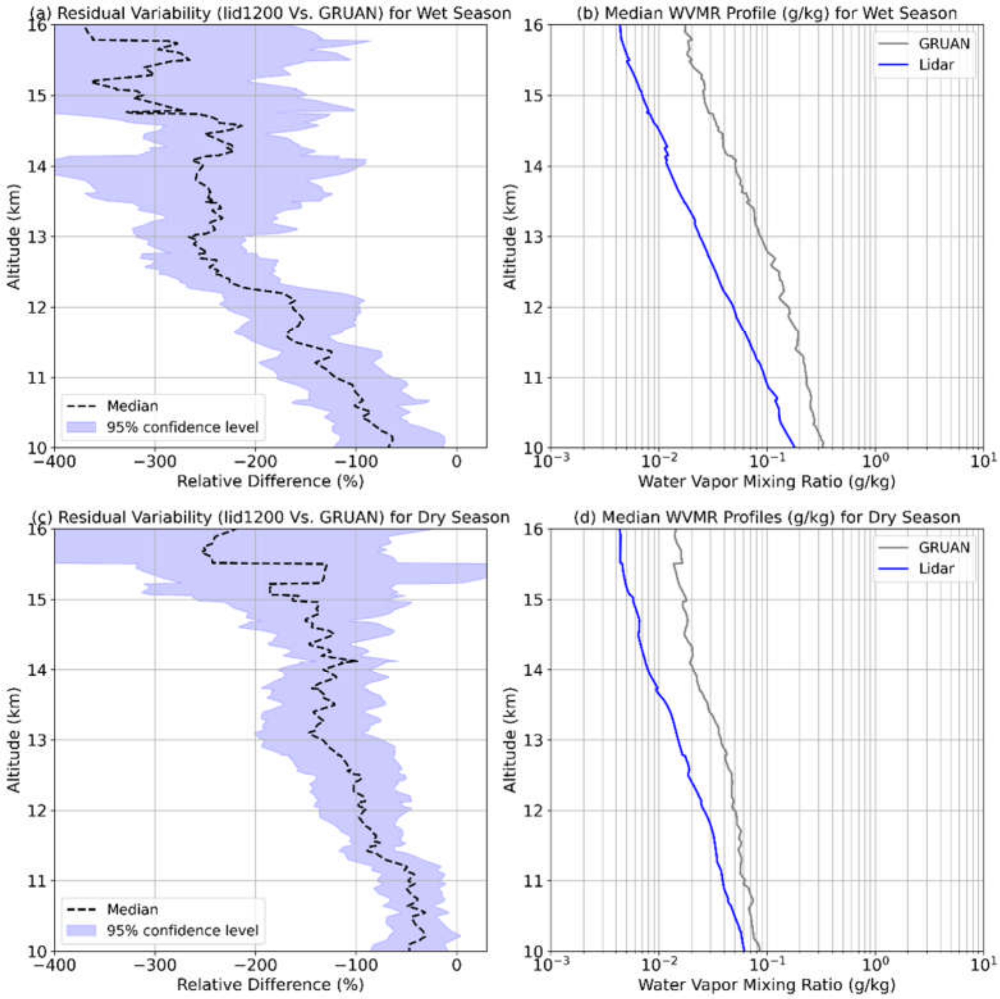

Figure 12. a) Median Lidar WVMR relative bias (%) w.r.t GRUAN during wet season months, (b) Median WVMR profile during the wet season (g/kg), (c) Median Lidar WVMR relative bias (%) w.r.t GRUAN during dry season months, (d) Median WVMR profile during the dry season (g/kg) , all over the 2013 to 2023 study period. Shaded zones refine the 95% confidence level median error.

4.4. Perspectives

Our results show a satellite MLS UT dry bias w.r.t Raman Lidar Water vapour mixing ratio profiles at pseudo-monthly scales. However, Raman Lidar is still slightly drier than ERA5 and clearly much drier than GRUAN analysed M10 radiosondes. Here, the question to be discussed is: How accurate is Raman Lidar observations of the upper tropospheric water vapor by the UV (355 nm emission as those by Lid1200) over the subtropics, in other words are they affected by the impact of the aerosols fluorescence previoulsy discussed by (Chouza et al., 2022) [38] over the same site and for the same lidar which is reported to produce wet lidar values, and this might explain MLS dry biases. If this is the case, Raman lidar is yet not sufficently wet compared to ERA5 and more compared to GRUAN M10 radiosondes, but what if GRUAN analysed M10 is located too far to be fairely compared, and the launched radiosondes might be also ecarted towards oceanic zones in the opposite direction from the site and hence sounding a far away vertical profile that not sufficiently close to be comparable?, We investigated this hypothysis, as shown in Figure 13, the radiosonde trajectories predominantly drift up to 100 km toward the East/Southern East from the Saint-Denis port, Figure 13 shows only the radiosondes drifts at altitudes between 10 and 16 km. A comparative analyse of the bias based on two classes of GRUAN M10 sounds drifts (near and far from the lidar location) is carried out, where results doesn't confirm any significant vertical/horizenatl drift effect (not shown).

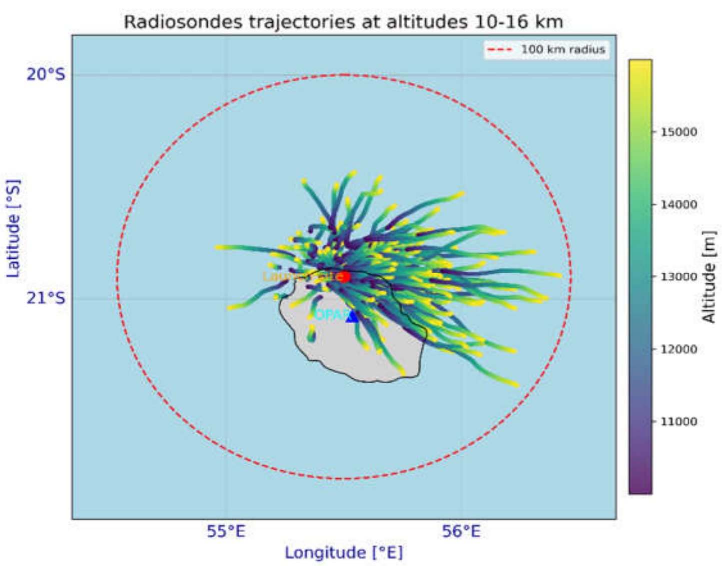

Figure 13. Trajectories of radiosondes launched from Saint-Denis port (red point at the Réunion Island) at altitudes 10–16 km. The color of each trajectory corresponds to the altitude. The red dashed circle indicates a 100 km radius around the launch site. The triangle marks the OPAR observatory (Lidar location).

Another interpretation is that the Raman lidar may *not* be significantly affected by fluorescence, and therefore does not exhibit a wet bias. In this scenario, MLS is really dry at the UT as previously reported by previous studies for MLS [21,22,35]. Concerning ERA5, it has been reported by divers efforts that ERA5 under-estimates humidity content at ice-supersaturation events (most frequent at

 doi:10.20944/preprints202602.1252.v1

the UT altitudes). Comparaisons with IAGOS observations, confirm that ERA5 tends to produce drier relative humidity variables at the UT altitudes, prompting several correction approaches [39,40]. But, our current operational Lidar dataset seemed even drier than ERA5 as demonstrated by the results of this section (4.2), especially during the dry season. These results challenge us to discuss a further perspective concerns the sensitivity of Raman lidar UT retrievals to calibration methodology. To investigate this aspect, we had genertaed a newly lidar WVMR dataset, using a different calibration method to be detailled in the follwoing section and most comparisons are investigated again w.r.t this new dataset.

5. Alternative Lidar Calibration

In this section, we present a novel calibration strategy, building upon the methodology introduced by (Alraddawi et al., 2025) [41]. Unlike the conventional approach, which relies on GNSS-derived Integrated Water Vapour (IWV) content as an external calibration reference [26], our method leverages the European Reanalysis ERA5 Water Vapour Mixing Ratio (WVMR) product.

5.1. Lidar1200-New Calibration Method

Specifically, within the new method, we focus on a narrow altitude band—between 4 and 6 km—to derive the calibration coefficients.

The selection of this altitude range is grounded in prior comparative analyses. By examining ERA5 midnight profiles against GRUAN-processed M10 radiosonde launches over Réunion Island, we identified the 4–6 km range as exhibiting the strongest agreement, with minimal bias between the two datasets.

The calibration started by the construction of a lidar-like pseudo-nightly ERA5 profiles, each of which is extracted from the 37 pressure levels ERA5 hourly dataset [19] by including only lidar-like nighttime observations. This pseudo-nightly product serves as our external calibration reference.

Following the framework established by [41] (Alraddawi et al., 2025), we derive nightly calibration factors and identify stable periods based on statistical approaches. These factors are then generalized to calibrate the entire 2013–2023 lidar nighttime dataset. we hence obtain new calibration coefficient with comparable values to those obtained by [26](Vérèmes et al., 2019). Figure 14 offers a comparative visualization of the generalized calibration factors obtained using both the traditional method (Vérèmes, 2019) and our new approach (Alraddawi, 2025). This comparison highlights the consistency between both calibration approaches, providing insights into respective uncertainties and performance under similar atmospheric conditions.

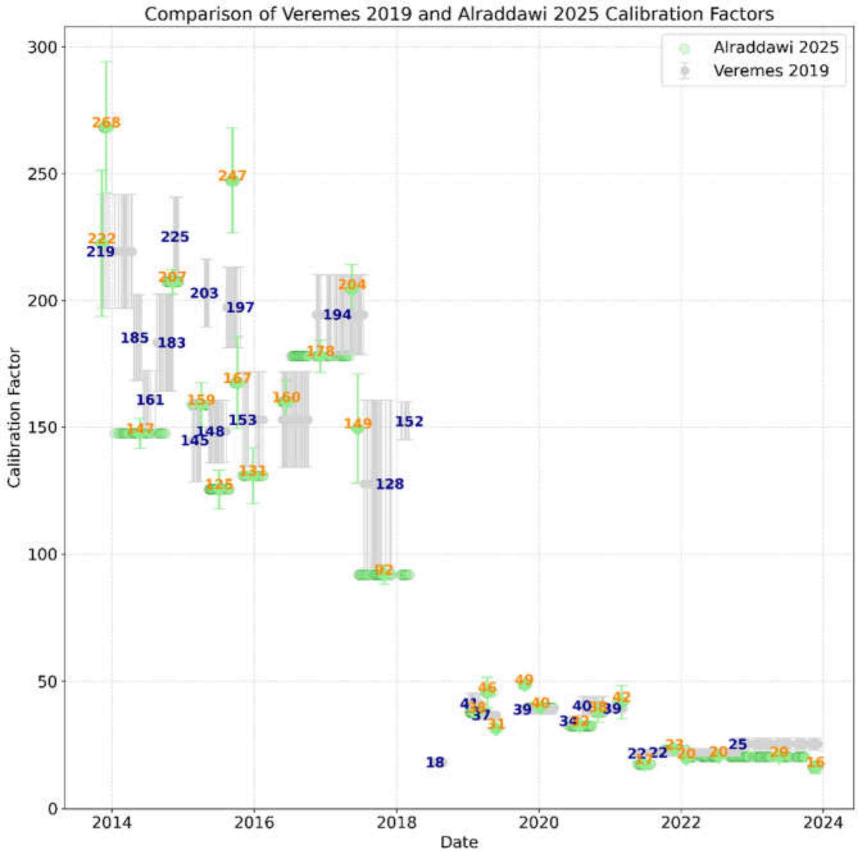

Figure 14. Final WVMR nightly calibration factors to be generalised according to their respective stable periods over 2013–2023, derived from the Vérèmes 2019 (grey and annotated in bleu marine); and Alraddawi 2025 (green and annotated in orange) methods. The plot displays median calibration factors with associated error bars for both methods over the observation period. Whiskers refer to the respective error at the 95% confidence leve.

Using the calibrated nightly dataset, we construct pseudo-monthly profiles, enabling a comparative analysis similar to that presented in Section 4. This newly generated dataset—referred to as *lid1200 new* in the accompanying figures—is then evaluated alongside established datasets, including ERA5, and GRUAN.

Our findings indicate that the Raman lidar *lid1200* WVMR datasets, regardless of the calibration method applied, remain consistent with one another. However, the *lid1200 new* dataset, exhibits slightly higher water vapour mixing ratios compared to the operational *lid1200* dataset, this difference is illustrated in Figure 15, where the median profiles of both datasets are compared.

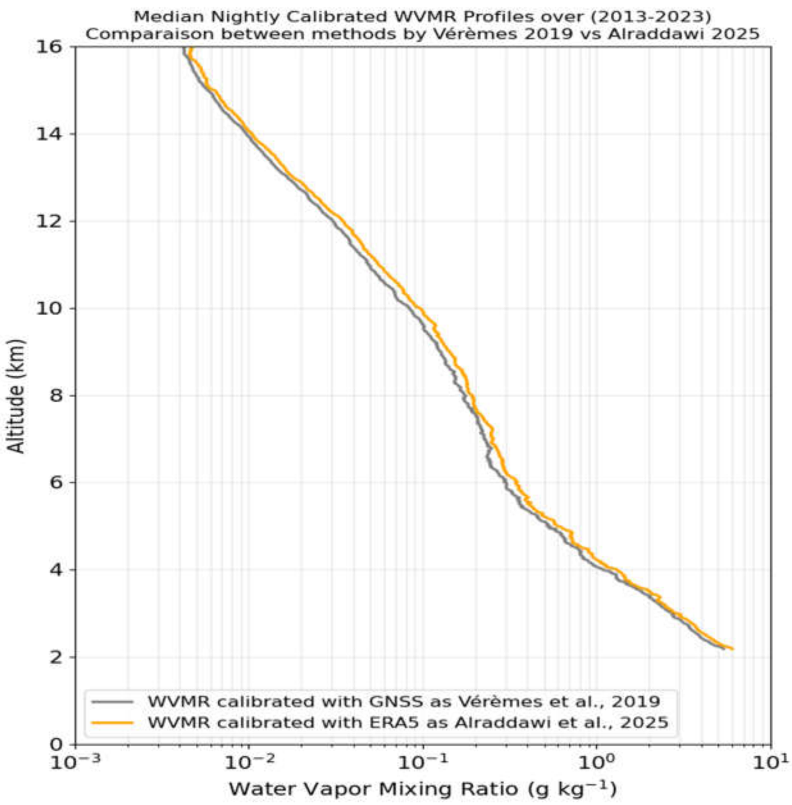

Figure 15. Median WVMR profile over the 2013-2023 period from both calibration methods.

5.2. Lidar1200-New vs ERA5

Going back to section 4.2, the median Lidar (vérèmes et al., 2019) bias w.r.t ERA5 didn't dépasse 5% at the upper troposphère with a drier than ERA5 altitudes (Figure 8). Carriying out the same comparison but using this time the lid1200 new dataset, we do report that the newly developped lidar datset are clearly more humide than ERA5 over the whole UT altitudes (Figure 16). Consequently we report a clear ERA5 dry bias all over the UT altitudes, can reach 20%. Similar ERA5 dry bias was reported by the authors over the Midlatitude [41]: up to 20% when ERA5 is compared to lidar WVMR calibrated the same way as the lid1200 new datasets, there study discussed and validated this bias by highlighting also the potential of a partial correction by IAGOS-MOZAIC observations, which are not available to be compared within our current study.

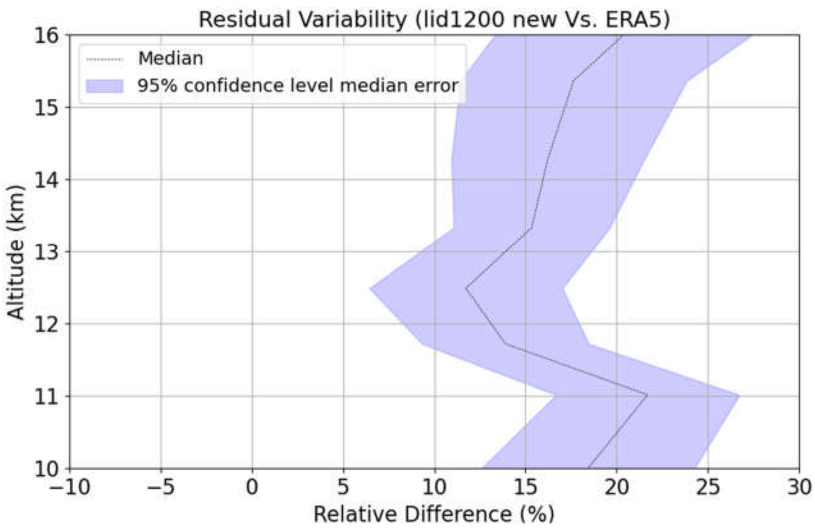

Preprints.org (www.preprints.org) | NOT PEER-REVIEWED | Posted: 17 February 2026 doi:10.20944/preprints202602.1252.v1

Figure 16. (Median Lidar (new) WVMR relative bias (%) w.r.t ERA5, from 2013 to 2023, shaded zones refine the 95% confidence level of the relative error;.

The seasonal analysis confirms the observed ERA5 dry bias up to 20% w.r.t lidar, with increased amplitude with altitude during the dry season (Figure 17). This might be due to ERA5 under-estimation of UT humidity (as demonstrated in the perspectives section 4.4), Also, the new lidar calibration enhancement of lidar humidity at the UT, and hence generating higher values compared to ERA5, which seemed to overcome previous calibration-related issue observed at the dry season (Figure 10,c) using the old calibration methode.

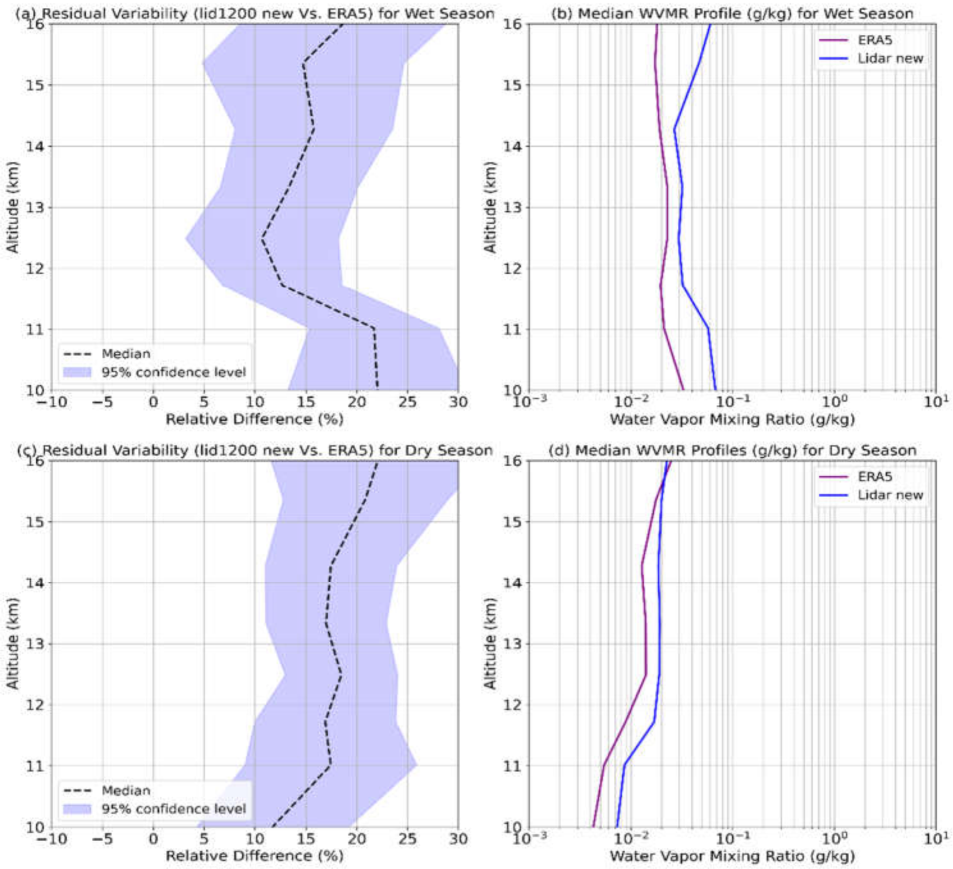

Figure 17. a) Median Lidar WVMR (new) relative bias (%) w.r.t ERA5 during wet season months, (b) Median WVMR (new) profile during the wet season (g/kg), (c) Median Lidar WVMR (new) relative bias (%) w.r.t ERA5 during dry season months, (d) Median WVMR (new) profile during the dry season (g/kg) , all over the 2013 to 2023 study period. Shaded zones refine the 95% confidence level median error.

5.3. Lidar1200-New vs GRUAN-M10 Processed

The lidar new dataset pseudo-monthlys exhibits also a pronounced dry bias w.r.t GRUAN-M10 processed dataset, exceeding 100% above 12 km and approaching 150% between 13 and 14 km, while remaining around 40% below 11 km (Figure 18). We do report a smaller Lidar WVMR dry bias w.r.t GRUAN M10 when the comparison concerns the Lidar WVMR new dataset (Figure 18), this reduced bias is notably noted at the UT altitudes, where the bias are reduced by about 50 % (mostly above 12 km) compared to the case when GRUAN is compared to Lidar WVMR operational dataset [26] (i.e calibrated with GNSS (See Figure 11)) Based on this, a small part of the operational lidar product dry bias w.r.t GRUAN (Figure 11) might be attributed to the current used operational calibration strategy, which might be generating drier Lidar WVMR profiles than reality due to the fact that this calibration method depends on the GNSS relaibility over this subtropical site. Some previous studies have reported a GNSS dry bias over the Réunion when compared to radiosondes(Bosser et al., 2022) [42].

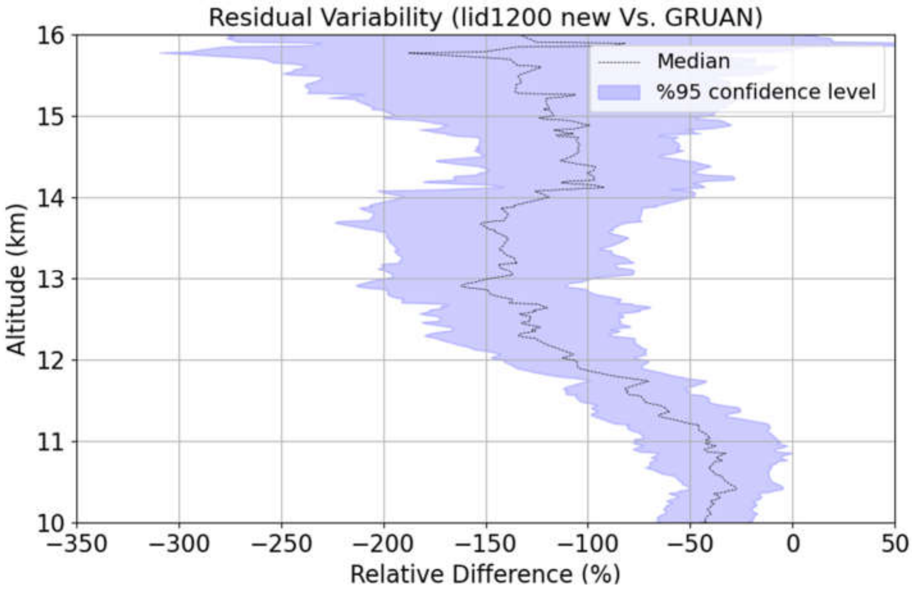

Figure 18. Median Lidar WVMR (new) relative bias (%) w.r.t GRUAN M10, (over 41 compared profiles from 2019 to 2023), shaded zones refine the 95% confidence level of the relative error.

Seasonal analysis reveals clear differences between the wet and dry periods (Figure 19). During the wet season, the variability is larger, with biases frequently around 200% above 13 km. During the dry season, the median bias is reduced, approximately 40% below 11 km and rising to 80% upwards. This analyse reports a clear reduced lidar dry bias w.r.t GRUAN during the dry season with the new calibration, if compared to the operational calibration (Figure 12), the dry bias is reduced more than 50%.

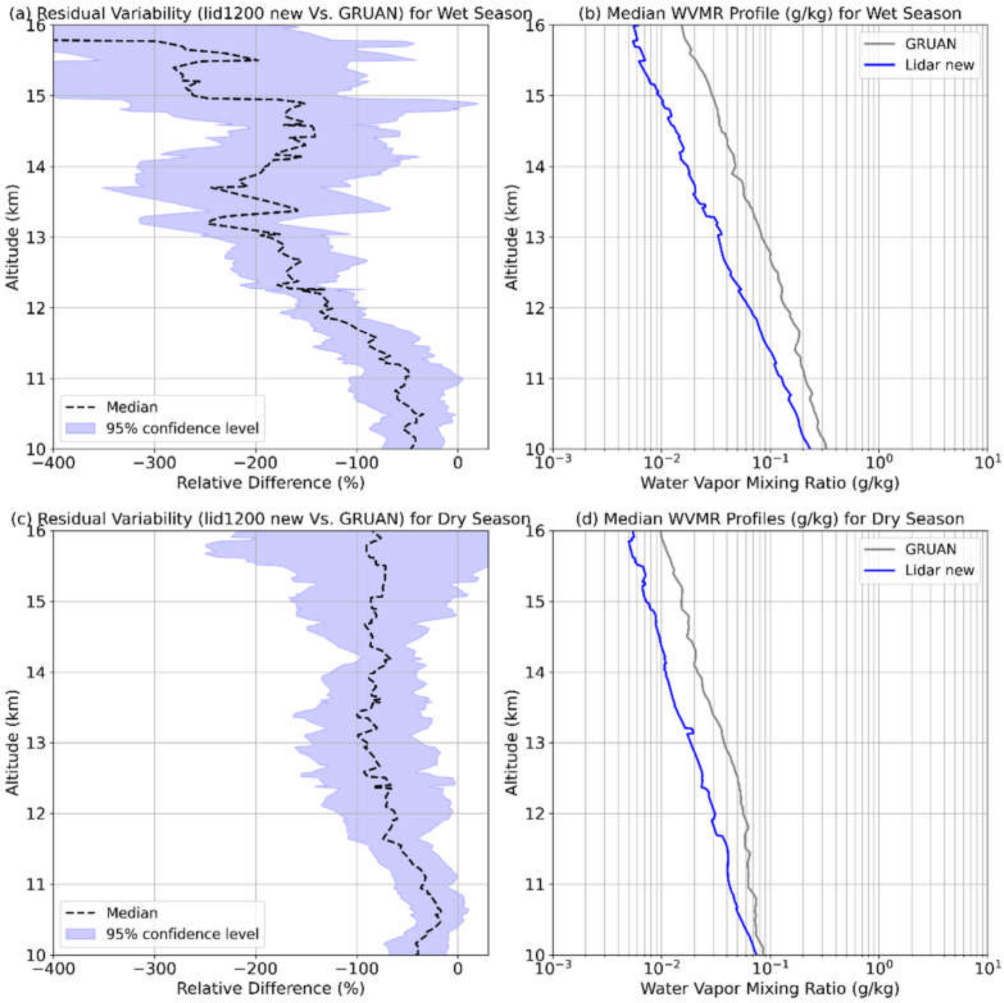

Figure 19. a) Median Lidar WVMR (new) relative bias (%) w.r.t GRUAN-M10 processed radiosondes during wet season months, (b) Median WVMR (new) profile during the wet season (g/kg), (c) Median Lidar WVMR (new) relative bias (%) w.r.t GRUAN-M10 during dry season months, (d) Median WVMR (new) profile during the dry season (g/kg) , all over the 2013 to 2023 study period. Shaded zones refine the 95% confidence level median error.

Raman Lidar lid1200 new Pseudo-monthly WVMR record would enable interesting investigations of the UT humidity trends, making use of such a multi-years dataset (since 2013 up to now). Generally the above cited perspectives could be tested more deeply within an upcoming measurements campaign planned over the Reunion Island in order to test the effect of the different calibration strategy and to allow a better colocated radiosondes launches with GRUAN processing code. The current paper open the door to such investigations via statistical analyse and open questions.

6. Conclusions

Valuable information about humidity content at the upper troposphere are possibly obtained by Satellites like MLS, re-analysis (ERA5) at global scales and more locally by Radiosondes referenced sources (like GRUAN), and Raman Lidar. But, accurate UT WVMR measurements are challenging, mostly above some less known regions like the subtropics. 11 years of WVMR profiles derived by those different data sources were analysed and statistically compared over the Reunion island between 2013 to 2023. Pseudo monthly screening was adopted to enhance the Lidar signal and obtain WVMR profiles up to the subtropical upper troposphere, this would also overcome the small number of the satellite MLS colocated overpasses at smaller scales. The comparison methode is then generated for all other compared datasets.

The muli-comparison at pseudo-monthly scale shows:

1. MLS exhibits dry bias w.r.t Lidar can reach 30% at the UT, particularly above 12 km and during the wet season. This dry MLS bias is consistent with findings reported in previous studies, such as [22] ; [35] which also have observed a significant dry bias of MLS WVMR compared to lidar in the upper troposphere.

2. ERA5 seemed to have closer to lidar values of WVMR at the UT values, small lidar dry bias doesn't exceed 5% is reported, more obviously during the dry season(up to 10%). However, Lidar newly developped dataset (calibrated as in Alraddawi et al., 2025) shows ERA5 dry bias with (up to 20% during the dry season). Similar ERA5 dry bias was previously reported over midlatitudes upper troposphere [40] ; [39] ; [41]. Over this subtropial site: this bias becomes more noticeable above 14 km.

3. Raman Lidar lid1200 demonstrates an important dry bias w.r.t GRUAN analysed M10 radiosondes. This bias is apparently not affected by radiosondes missmatching (misscollocation) of the airmass due to radiosondes derivation from the zenith over the launch site where they could be derived up to 100 km far away. However, Lid1200 dataset could be much drier than reality being calibrated via GNSS IWV quantities which is reported previously to be driely biased over the Reunion island w.r.t radiosondes [42]. This hypothesis was validated, based on a clearly reduced lidar dry bias w.r.t GRUAN-processed M10 radiosondes when the new lidar (lid1200 new) dataset (calibrated differently) was compared, and much lower bias during the dry season (30-80%).

In conclusion, Raman Lidar technique seemed more sensetive than MLS in detecting humidity content at upper troposphere altitudes. Even though the current calibration strategy seemed to produce drier than reality profiles, follwoing the GNSS reference use. Hence, the current lidar datasets seemed much drier than GRUAN-referenced M10 dataset. And this important bias, seemed to be partially reduced with a different lidar calibration strategy but not totally removed/inversed and still important (30-100%). We do recomand deeper investigations about the possible sources of such a lidar bias, via an upcoming measurement campaign, which might help to further refine and extend the analysis to broader atmospheric conditions over this important subtropical region, and to open the door to the confident use of this dataset for the UT humidity trends .

Author Contributions: Conceptualization, P.K.; methodology, D.A. and A.H.; software, G.P. ; validation, P.K. and D.A.; formal analysis, D.A.; investigation, D.A., A.H., M. S. .; resources, P.K.; data curation, D.A. and G.P. ; writing—original draft preparation, D.A.; writing—review and editing, J-L. B. , F.M., A.H., A.I. and A.S.; visualisation, D.A.; supervision, P.K.; project administration, P.K.; funding acquisition, P.K. All authors have read and agreed to the published version of the manuscript.

Funding: This project has received funding from the Horizon Europe Research and Innovation Actions program under Grant Agreement N°101056885 through the BeCoM (Better Contrail Mitigation) project and from the French government (BPI) in the frame of France 2030 under Grant DOS0182433/00 for the CONTRAILS project.

Data Availability Statement: ERA5 data set are publicly available at: https://cds.climate.copernicus.eu/datasets/reanalysis-era5-pressure-levels?tab=download, last access: 11 February 2026, GRUAN-analysed M10 radiosondes dataset is from the IPSL climserv data server. MLS data are publicly available at: https://acdisc.gesdisc.eosdis.nasa.gov/data/Aura_MLS_Level2/ML2H2O.005/, last access: 11 February 2026,

Acknowledgments: The authors would like to thank the technical and IT staff of the lid1200 lidar. the authors would like to thank also Milena Martic (Grodien Strato co.) for the lidar expertise.

Conflicts of Interest: The authors declare no conflicts of interest.

References

1. L. Qian, J. Rao, R. Ren, C. Shi, et S. Liu, « Enhanced stratosphere-troposphere and tropics-Arctic couplings in the 2023/24 winter », *Commun Earth Environ*, vol. 5, nº 1, p. 631, oct. 2024, doi: 10.1038/s43247-024-01812-x.
2. A. Gettelman et Q. Fu, « Observed and Simulated Upper-Tropospheric Water Vapor Feedback », *Journal of Climate*, vol. 21, nº 13, p. 3282-3289, juill. 2008, doi: 10.1175/2007JCLI2142.1.
3. A. E. Dessler, Z. Zhang, et P. Yang, « Water-vapor climate feedback inferred from climate fluctuations, 2003–2008 », *Geophysical Research Letters*, vol. 35, nº 20, p. 2008GL035333, oct. 2008, doi: 10.1029/2008GL035333.
4. R. Colman et B. J. Soden, « Water vapor and lapse rate feedbacks in the climate system », *Rev. Mod. Phys.*, vol. 93, nº 4, p. 045002, nov. 2021, doi: 10.1103/RevModPhys.93.045002.
5. X. Wang et A. E. Dessler, « The response of stratospheric water vapor to climate change driven by different forcing agents », *Atmos. Chem. Phys.*, vol. 20, nº 21, p. 13267-13282, nov. 2020, doi: 10.5194/acp-20-13267-2020.
6. V. Wulfmeyer et al., « A review of the remote sensing of lower tropospheric thermodynamic profiles and its indispensable role for the understanding and the simulation of water and energy cycles », *Reviews of Geophysics*, vol. 53, nº 3, p. 819-895, sept. 2015, doi: 10.1002/2014RG000476.
7. E. J. Fetzer et al., « Comparison of upper tropospheric water vapor observations from the Microwave Limb Sounder and Atmospheric Infrared Sounder », *J. Geophys. Res.*, vol. 113, nº D22, p. 2008JD010000, nov. 2008, doi: 10.1029/2008JD010000.
8. W. G. Read et al., « Aura Microwave Limb Sounder upper tropospheric and lower stratospheric H_2O and relative humidity with respect to ice validation », *J. Geophys. Res.*, vol. 112, nº D24, p. 2007JD008752, déc. 2007, doi: 10.1029/2007JD008752.
9. W. G. Read et al., « The SPARC Water Vapor Assessment II: assessment of satellite measurements of upper tropospheric humidity », *Atmos. Meas. Tech.*, vol. 15, nº 11, p. 3377-3400, juin 2022, doi: 10.5194/amt-15-3377-2022.
10. J. W. Waters et al., « The Earth observing system microwave limb sounder (EOS MLS) on the aura Satellite », *IEEE Transactions on Geoscience and Remote Sensing*, vol. 44, nº 5, p. 1075-1092, mai 2006, doi: 10.1109/TGRS.2006.873771.
11. S. M. Davis et al., « Validation of SAGE III/ISS Solar Water Vapor Data With Correlative Satellite and Balloon-Borne Measurements », *JGR Atmospheres*, vol. 126, nº 2, p. e2020JD033803, janv. 2021, doi: 10.1029/2020JD033803.
12. M. I. Hegglin et al., « SPARC Data Initiative: Comparison of water vapor climatologies from international satellite limb sounders », *JGR Atmospheres*, vol. 118, nº 20, oct. 2013, doi: 10.1002/jgrd.50752.
13. H. Vömel, D. E. David, et K. Smith, « Accuracy of tropospheric and stratospheric water vapor measurements by the cryogenic frost point hygrometer: Instrumental details and observations », *J. Geophys. Res.*, vol. 112, nº D8, p. 2006JD007224, avr. 2007, doi: 10.1029/2006JD007224.
14. H. Vömel, T. Naebert, R. Dirksen, et M. Sommer, « An update on the uncertainties of water vapor measurements using cryogenic frost point hygrometers », *Atmos. Meas. Tech.*, vol. 9, nº 8, p. 3755-3768, août 2016, doi: 10.5194/amt-9-3755-2016.
15. M. Fujiwara et al., « Seasonal to decadal variations of water vapor in the tropical lower stratosphere observed with balloon-borne cryogenic frost point hygrometers », *J. Geophys. Res.*, vol. 115, nº D18, p. 2010JD014179, sept. 2010, doi: 10.1029/2010JD014179.
16. R. J. Dirksen et al., « Managing the transition from Vaisala RS92 to RS41 radiosondes within the Global Climate Observing System Reference Upper-Air Network (GRUAN): a progress report », *Geoscientific Instrumentation, Methods and Data Systems*, vol. 9, nº 2, p. 337-355, 2020.
17. D. Sperber et K. Gierens, « Towards a more reliable forecast of ice supersaturation: concept of a one-moment ice-cloud scheme that avoids saturation adjustment », *Atmospheric Chemistry and Physics*, vol. 23, nº 24, p. 15609-15627, 2023.
18. H. Hersbach et al., « The ERA5 global reanalysis », *Quarterly Journal of the Royal Meteorological Society*, vol. 146, nº 730, p. 1999-2049, 2020.
19. H. Hersbach et al., « ERA5-hourly data on model levels, ECMWF [data set] ». 2023.

20. P. Konjari et al., « Technical note: Water vapour climatologies in the extra-tropical upper troposphere and lower stratosphere derived from a synthesis of passenger and research aircraft measurements », *Atmos. Chem. Phys.*, vol. 25, nº 7, p. 4269-4289, avr. 2025, doi: 10.5194/acp-25-4269-2025.
21. T. Leblanc, I. McDermid, et T. Walsh, « Ground-based water vapor Raman lidar measurements up to the upper troposphere and lower stratosphere for long-term monitoring », *Atmospheric Measurement Techniques*, vol. 5, nº 1, p. 17-36, 2012.
22. D. Dionisi et al., « Water vapor observations up to the lower stratosphere through the Raman lidar during the Maïdo Lidar Calibration Campaign », *Atmospheric Measurement Techniques*, vol. 8, nº 3, p. 1425-1445, 2015.
23. O. Bock et al., « Accuracy assessment of water vapour measurements from in-situ and remote sensing techniques during the DEMEVAP 2011 campaign at OHP », *Atmospheric Measurement Techniques Discussions*, vol. 6, nº 2, p. 3439-3509, 2013.
24. J.-L. Baray et al., « Maïdo observatory: a new high-altitude station facility at Reunion Island (21° S, 55° E) for long-term atmospheric remote sensing and in situ measurements », *Atmospheric Measurement Techniques*, vol. 6, nº 10, p. 2865-2877, oct. 2013, doi: 10.5194/amt-6-2865-2013.
25. P. Keckhut et al., « Introduction to the Maïdo Lidar Calibration Campaign dedicated to the validation of upper air meteorological parameters », *JARS*, vol. 9, nº 1, p. 094099, avr. 2015, doi: 10.1117/1.JRS.9.094099.
26. H. Vérèmes et al., « Validation of the water vapor profiles of the raman lidar at the maïdo observatory (Reunion Island) calibrated with global navigation satellite system integrated water vapor », *Atmosphere*, vol. 10, nº 11, p. 713, 2019.
27. V. Sherlock, A. Garnier, A. Hauchecorne, et P. Keckhut, « Implementation and validation of a Raman lidar measurement of middle and upper tropospheric water vapor », *Applied Optics*, vol. 38, nº 27, p. 5838-5850, 1999.
28. P. Keckhut, M.-L. Chanin, et A. Hauchecorne, « Stratosphere temperature measurement using Raman lidar », *Applied optics*, vol. 29, nº 34, p. 5182-5186, 1990.
29. T. Leblanc et al., « Proposed standardized definitions for vertical resolution and uncertainty in the NDACC lidar ozone and temperature algorithms – Part 1: Vertical resolution », *Atmos. Meas. Tech.*, vol. 9, nº 8, p. 4029-4049, août 2016, doi: 10.5194/amt-9-4029-2016.
30. N. J. Livesey, W. Van Snyder, W. G. Read, et P. A. Wagner, « Retrieval algorithms for the EOS Microwave limb sounder (MLS) », *IEEE Transactions on Geoscience and Remote Sensing*, vol. 44, nº 5, p. 1144-1155, mai 2006, doi: 10.1109/TGRS.2006.872327.
31. A. Lambert et al., « Validation of the Aura Microwave Limb Sounder middle atmosphere water vapor and nitrous oxide measurements », *J. Geophys. Res.*, vol. 112, nº D24, p. 2007JD008724, déc. 2007, doi: 10.1029/2007JD008724.
32. H. Vömel et al., « Validation of Aura Microwave Limb Sounder water vapor by balloon-borne Cryogenic Frost point Hygrometer measurements », *J. Geophys. Res.*, vol. 112, nº D24, p. 2007JD008698, déc. 2007, doi: 10.1029/2007JD008698.
33. G. Berthet, J.-B. Renard, M. Ghysels, G. Durry, B. Gaubicher, et N. Amarouche, « Balloon-borne observations of mid-latitude stratospheric water vapour: comparisons with HALOE and MLS satellite data », *J Atmos Chem*, vol. 70, nº 3, p. 197-219, sept. 2013, doi: 10.1007/s10874-013-9264-7.
34. D. F. Hurst et al., « Validation of Aura Microwave Limb Sounder stratospheric water vapor measurements by the NOAA frost point hygrometer », *JGR Atmospheres*, vol. 119, nº 3, p. 1612-1625, févr. 2014, doi: 10.1002/2013JD020757.
35. X. Yan, J. S. Wright, X. Zheng, N. J. Livesey, H. Vömel, et X. Zhou, « Validation of Aura MLS retrievals of temperature, water vapour and ozone in the upper troposphere and lower–middle stratosphere over the Tibetan Plateau during boreal summer », *Atmospheric Measurement Techniques*, vol. 9, nº 8, p. 3547-3566, août 2016, doi: 10.5194/amt-9-3547-2016.
36. D. J. Seidel et al., « Reference Upper-Air Observations for Climate: Rationale, Progress, and Plans », *Bulletin of the American Meteorological Society*, vol. 90, nº 3, p. 361-369, mars 2009, doi: 10.1175/2008BAMS2540.1.

37. J.-C. Dupont, M. Haeffelin, J. Badosa, G. Clain, C. Raux, et D. Vignelles, « Characterization and corrections of relative humidity measurement from Meteomodem M10 radiosondes at midlatitude stations », *Journal of Atmospheric and Oceanic Technology*, vol. 37, nº 5, p. 857-871, 2020.
38. F. Chouza et al., « The impact of aerosol fluorescence on long-term water vapor monitoring by Raman lidar and evaluation of a potential correction method », *Atmospheric Measurement Techniques*, vol. 15, nº 14, p. 4241-4256, juill. 2022, doi: 10.5194/amt-15-4241-2022.
39. S. Hofer, K. Gierens, et S. Rohs, « How well can persistent contrails be predicted? An update », *Atmos. Chem. Phys.*, vol. 24, nº 13, p. 7911-7925, juill. 2024, doi: 10.5194/acp-24-7911-2024.
40. K. Wolf, N. Bellouin, O. Boucher, S. Rohs, et Y. Li, « Correction of temperature and relative humidity biases in ERA5 by bivariate quantile mapping: Implications for contrail classification », *EGUsphere*, vol. 2023, p. 1-38, 2023.
41. D. Alraddawi et al., « Calibration of Upper Air Water Vapour Profiles Using the IPRAL Raman Lidar and ERA5 Model Results and Comparison to GRUAN Radiosonde Observations », *Atmosphere*, vol. 16, nº 3, p. 351, mars 2025, doi: 10.3390/atmos16030351.
42. P. Bosser, J. Van Baelen, et O. Bousquet, « Routine Measurement of Water Vapour Using GNSS in the Framework of the Map-Io Project », *Atmosphere*, vol. 13, nº 6, p. 903, juin 2022, doi: 10.3390/atmos13060903.